KSME

Springer

Journal of Mechanical Science and Technology 37 (7) 2023

Original Article
DOI 10.1007/s12206-023-0605-4

Keywords:
· Roller opposite force
· Tire modeling
· Brake tester simulation
· Braking efficiency
· Tire testing
· Advantages disadvantages of roller brake tester
· Twin-roller chassis dynamometer

Correspondence to:
Ery Muthoriq
ery.2002@gmail.com

Citation:
Muthoriq, E., Abidin, Z., Hariyanto, A., Bur, M. (2023). Enhancement of a roller brake tester for modelling the tire. Journal of Mechanical Science and Technology 37 (7) (2023) 3379~3391.
http://doi.org/10.1007/s12206-023-0605-4

Received September 28th, 2022
Revised February 6th, 2023
Accepted March 10th, 2023

† Recommended by Editor
No-cheol Park

Enhancement of a roller brake tester for modelling the tire

Ery Muthoriq[1], Zainal Abidin[1], Arief Hariyanto[1] and Mulyadi Bur[2]

[1]Department of Mechanical Engineering, Faculty of Mechanical and Aerospace Engineering, Institut Teknologi Bandung, Bandung 40132, Indonesia, [2]Department of Mechanical Engineering, Faculty of Engineering, Universitas Andalas, Padang 25163, Indonesia

Abstract A tire model can be used to predict vehicle dynamics behaviour, such as braking or turning. This paper proposes a method for testing/modelling a tire with a roller brake tester. It requires two speed sensors installed on the roller and idler. That additional sensors are used to estimate roller brake tester inertia and measure tire slip during testing. After involving inertia in the calculation, the brake tester measurement becomes accurate in all points from zero until maximum slip. These results are better than the existing roller brake tester which is only accurate when the steady state condition of the roller is achieved. The modified brake tester and tire testing were modelled and simulated using MATLAB® Simulink. Furthermore, the influence of the brake tester arrangement on measurement characteristics has been identified.

1. Introduction

In the last few years, there has been a lot of research on traffic safety, especially in the braking system of a vehicle [1-3]. It is generally accepted that the vehicle braking performance depends on the braking torque and tire-road friction force [4]. Braking torque is caused by the friction between the brake pad and the disc for the disk brake or the brake shoe and the drum for the drum brake. Meanwhile, the tire-road friction force is caused by tire thread deformation generating a phenomenon called slip.

Slip characteristics of a tire influence the tire-road friction force and show the relationship between friction force and slip. They are often modelled with Julien's theory, magic formula, or brush model. Julien's theory is one of the earliest tire models assuming that the contact patch is a rectangle and the pressure is uniformly distributed [5, 6]. Magic formula is the most frequently used today for modelling longitudinal force, lateral force and aligning torque [7, 8]. Unlike magic formula, an empirical model, brush model has been made based on the physical interaction between the tire tread and the road. As a result, transient brush and out-of-plane flexible ring tire models are still being developed [9-11].

There are some advantages if the tire model is known. Tires from different manufacturers can be compared because parameters in tire models are influenced by their stiffness and operating condition, such as normal load, inflation pressure, wear rate, and speed [12]. The tire model also can be used to determine the vehicle's dynamic behaviour, such as in braking or turning manoeuvres [13-16]. Furthermore, the tire model can be used for designing braking control systems because it will contribute to antilock braking system (ABS) performance [17].

Modelling the tire requires experiment data from tire testing. Data required are tire-road friction force from 0 % slip (free rolling) until 100 % slip (locking). Tire testing can be classified into two categories: laboratory and drive tests. The laboratory uses a flat road or drum testing machine [18]. Operating conditions such as speed, normal load, and inflation pressure can be varied easily. For a drive test, a vehicle is driven at a certain speed, and then the driver brakes it until the tire locks (100 % slip). A dynamometric rim is attached to the wheel to measure longitudinal force, normal force, and angular velocity [19]. To calculate slip, the angular velocity of

the vehicle wheel is compared with the angular velocity of the fifth wheel pulled by the vehicle in free-rolling conditions [20]. The laboratory test is expensive because the number of those testing machines is limited. Only a special laboratory has that testing facility. On the other hand, the drive test also has weaknesses, such as requiring a long track, taking more time, and being difficult to perform.

A roller brake tester can be used as an alternative device for tire testing, which is cheaper and easy to use, although it requires some modifications. Unlike flat road or drum testing machines, the roller brake tester can easily be found in every city in a vehicle periodic inspection office. However, it has some weaknesses that must be solved before it can be used as a tire tester. First, a roller brake tester only measures one parameter, that is, maximum friction force/maximum friction coefficient/maximum braking efficiency. Meanwhile, tire modelling requires data on various friction forces from free rolling until locking. Second, its measurement is affected by an angle β. That angle is formed because of the distance between rollers, roller diameter, and tire radius. The same vehicle will have different braking efficiency if tested on other brake testers with different angles β. The bigger the angle, the higher the braking efficiency is [21-25]. Third, the inertia of the brake tester components, such as rollers, gearbox, and transmission system will be responsible for measurement inaccuracy [26]. An experiment shows that a roller brake tester has a measurement error up to 10.4 % [27]. Since tire testing must be done from free rolling until locking, the device should be accurate in all conditions for both transient and steady-state conditions. Therefore, it needs modification to make the roller brake tester capable of testing a tire.

There are some developments in the roller brake tester. It is introduced in 1937 [28]. At that time, it still used mechanical sensors and displays. Nowadays, because of the advent of computers, modern technology components such as electronic sensors, analog-to-digital converter (ADC) modules, personal computers for signal processing, monitor display, printer, etc., have been used [29]. For testing ABS (antilock brake system), a control circuit that commands the modulator to increase, hold, and decrease the hydraulic pressure has been introduced [30]. The braking force of those three modes is measured by a roller brake tester. To make the tire contact patch similar to when it stands on flat ground, a belt is installed between two rollers [31]. The assembly of those rollers and belt is supported by sensors measuring normal, longitudinal, and lateral force. Hence, the test rig arrangement becomes complicated. For safety purpose, a non-contact sensor (triangulation sensor) is introduced to detect whether the vehicle wheel is already on the test bench [32]. To reduce the influence of the angle β, a mechanism for setting the distance between two rollers is introduced [33]. If testing is performed for different sizes of tires, the distance between the roller needs to be adjusted. Based on those developments, no one has used the roller brake tester to characterize the tire.

Some researchers have proposed measurement methods to solve the roller brake tester weaknesses. To obtain braking force data in various friction coefficients (not only maximum braking force), a magnetic powder clutch, a flywheel, and a roller are used to simulate multiple friction coefficients, the vehicle speed, and the wheel speed [34]. To attach a sensor as close as possible to the roller surface, a non-contact sensor (magneto strictive sensor) is installed on the roller shaft [35]. To avoid the existence of angle β and the inertia, a static brake tester using a slowly moving plate is proposed [36]. To measure braking force accurately, a sensor is installed on the brake pad, the calliper, or the hydraulic circuit of the braking system [37-40].

Improvements had been done above can increase the measurement accuracy. However, if those methods are applied in the existing roller brake tester, it will require many modifications. Therefore, the cost is expensive. Furthermore, if we use sensors installed on the vehicle wheel or braking system circuit, it becomes impractical to be applied in a vehicle inspection station. It takes time to install sensors on the vehicle.

The objective of this paper is to find a tire testing method using a roller brake tester with the simplest modification. Outputs of this modified brake tester are not only maximum braking efficiency but also tire model. Also, the cost is not expensive because it only needs a little modification, and that test rig has been used widely in the vehicle inspection facility. The purpose of the modification is to increase the measurement accuracy by taking the inertia of brake tester components into account and to obtain data for tire modelling, i.e., friction force and slip. The rotational inertia of a typical test rig (twin-roller chassis dynamometer) has been studied experimentally and in simulation [41, 42]. However, the scenario on the chassis dynamometer is acceleration, not braking. Moreover, in those studies, the inertia is estimated when the electric motor is controlled in constant acceleration. That method cannot be performed in a roller brake tester because it is not equipped with an inverter. In this paper, tire testing with the modified roller brake tester is modelled and simulated using MATLAB® Simulink.

This paper is organized as follows: in Sec. 2, modelling of a roller brake tester from electric motor, brake tester components, until tire characteristics are performed. From that modelling processes, advantages and weaknesses of a roller brake tester are identified; in Sec. 3, a method to enhance the measurement accuracy and sensors required are presented; Sec. 4 discuss simulation results of the existing and modified roller brake tester when they are used for testing/modelling the tire; conclusions are drawn in Sec. 5.

2. Modelling of a roller brake tester

Modelling was performed based on the working principle of a roller brake tester shown in Fig. 1(a). Power from an electric motor is delivered to the wheel through a pinion gear, ring gear, roller 1, and roller 2. Roller 2 is connected to roller 1 by a chain. The idler placed between two rollers is used for safety purpose. A switch is attached to the idler support. The electric motor can be started whenever this switch is pressed. Hence, when there

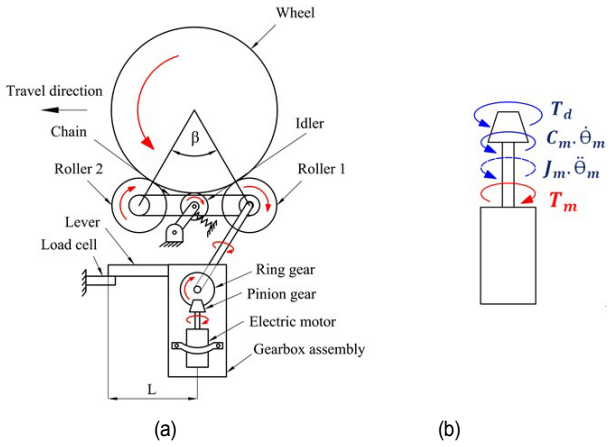

Fig. 1. (a) Schematic of a roller brake tester; (b) free body diagram of the electric motor.

is no vehicle wheel above the rollers, testing cannot be performed, although the operator presses the start button. In this paper, the idler was used not only for safety but also to measure the linear velocity of the wheel. That linear velocity was then used to measure the slip between the wheel and rollers.

The braking force or friction force between the tire and rollers is measured by a load cell. The load cell receives force from a lever attached to the gearbox assembly, as shown in Fig. 1(a). When the driver of a car being tested presses the brake pedal, the load cell measures the braking force. The maximum braking force divided by the normal force returns braking efficiency or maximum friction coefficient.

This section is divided into two sub-sections: modelling of each brake tester component and how to combine them. The components to be modelled consists of an electric motor, rollers, action force on the braked wheel, maximum and sliding friction force, and friction force at the roller surface. Combining those models with the gearbox model will result in a model of a brake tester.

2.1 Modelling of brake tester components

The electric motor model was made based on the free-body diagram in Fig. 1(b). An equation to calculate the acceleration of the electric motor shaft can be expressed as:

$$\ddot{\theta}_m = \frac{1}{J_m}\left(T_m - C_m.\dot{\theta}_m - T_d\right) \tag{1}$$

where $\ddot{\theta}_m$ is the acceleration of the electric motor shaft, T_m is the electric motor torque, J_m is the moment of inertia of the electric motor, C_m is viscous damping, and T_d is load torque.

The mechanical power output of the electric motor based on the nameplate is 11 kW at 2945 rpm. Hence, the electric motor torque can be calculated as follows:

$$T_m = \frac{11000\,Nm/s}{308.2\,rad/s} = 35.7\,Nm\,. \tag{2}$$

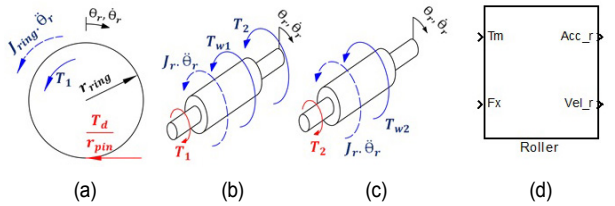

Fig. 2. Model of rollers: (a) free body diagram of the ring gear of the gearbox assembly; (b) free body diagram of roller 1; (c) free body diagram of roller 2; (d) subsystem of rollers.

To reach the synchronous speed (3000 rpm) in 0.3 s [43], with T_d = 0 and T_m = 35.7 Nm, using Eq. (1), it needs J_m = 0.001 kg.m^2 and C_m = 0.1137 N.m.s/rad. Those values will be applied to the brake tester simulation in Sec. 4.

The model of rollers was made based on the free body diagram of the ring gear in Fig. 2(a), roller 1 in Fig. 2(b), and roller 2 in Fig. 2(c). Hence, load torque T_d can be expressed as:

$$T_d = \frac{r_{pin}}{r_{ring}}\left(J_{ring} + 2.J_r\right)\ddot{\theta}_r + \frac{r_{pin}}{r_{ring}}\left(T_{w1} + T_{w2}\right) \tag{3}$$

where r_{pin} and r_{ring} are the effective radius of the pinion and ring gear, J_{ring} and J_r are the moment of inertia of the ring gear and roller, $\ddot{\theta}_r$ is the acceleration of the roller, T_{w1} and T_{w2} are torque because of friction on roller 1 and roller 2.

$$\text{Let: } T_{w1} + T_{w2} = F_x.r_r \tag{4}$$

where F_x is the total friction force between two rollers and the wheel and r_r is the roller radius.

Substituting Eqs. (3) and (4) in Eq. (1):

$$J_m.\ddot{\theta}_m + C_m.\dot{\theta}_m + \frac{r_{pin}}{r_{ring}}.\left(J_{ring} + 2.J_r\right).\ddot{\theta}_r + \frac{r_{pin}}{r_{ring}}.F_x \cdot r_r - T_m = 0\,. \tag{5}$$

The relationship between the speed of electric motor shaft $\dot{\theta}_m$ and rollers $\dot{\theta}_r$ can be expressed as:

$$\dot{\theta}_m = \frac{r_{ring}}{r_{pin}} \cdot \dot{\theta}_r \tag{6}$$

$$\text{Let: } J_{tot} = J_m.\frac{r_{ring}}{r_{pin}} + \frac{r_{pin}}{r_{ring}}.\left(J_{ring} + 2.J_r\right). \tag{7}$$

Substituting Eqs. (6) and (7) in Eq. (5):

$$J_{tot}.\ddot{\theta}_r + C_m.\frac{r_{ring}}{r_{pin}}.\dot{\theta}_r + \frac{r_{pin}}{r_{ring}}.F_x.r_r - T_m = 0\,. \tag{8}$$

Based on Eq. (8), a subsystem can be built, as shown in Fig. 2(d). This subsystem is called the roller subsystem. Building a subsystem is required to make a block diagram simple when it

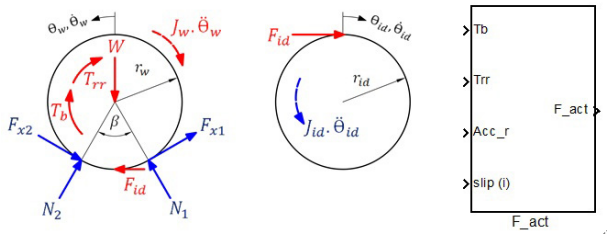

Fig. 3. Model of action force F_{act} on the tested wheel: (a) free body diagram of the wheel; (b) free body diagram of the idler; (c) the subsystem of action force F_{act} acting on the wheel.

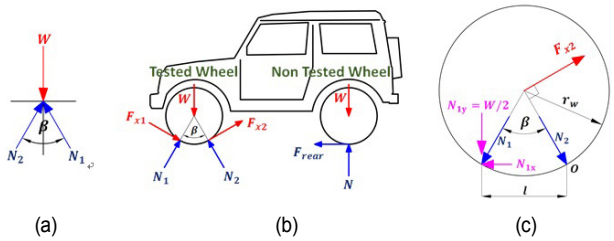

Fig. 4. Analysis of when the vehicle moves backwards while testing: (a) the normal force on rollers 1 and 2; (b) forces on tested and non-tested wheels; (c) free body diagram of the tested wheel to predict when the vehicle moves backwards.

needs to be connected with another block diagram or subsystem.

From Fig. 2(d), it can be seen that the unknown input is friction force F_x. That force is located on two rollers surface because of the braked wheel. To calculate F_x, it requires a free-body diagram of the wheel, as shown in Fig. 3(a).

From free body diagram of the wheel and idler, as shown in Figs. 3(a) and (b), an equation to calculate the action force acting on the wheel F_{act} can be derived as follows:

$$F_{act} = \frac{1}{r_w}.\left(T_b + T_{rr} + J_w.\ddot{\theta}_w + J_{id}.\frac{r_w}{r_{id}}.\ddot{\theta}_{id}\right) \tag{9}$$

where r_w and r_{id} are effective radius of the wheel and idler, T_b is braking torque, T_{rr} is rolling resistance torque, J_w and J_{id} are moment of inertia of the wheel and idler, $\ddot{\theta}_w$ is wheel acceleration, and $\ddot{\theta}_{id}$ is idler acceleration.

By assuming that there is no slip between the wheel and the idler, the wheel speed can be measured based on the idler speed with this equation:

$$\dot{\theta}_w = \frac{r_{id}}{r_w}.\dot{\theta}_{id}\,. \tag{10}$$

Because there is a slip between the vehicle wheel and rollers when the wheel is braked, the relationship between idler and roller can be expressed as:

$$\dot{\theta}_{id} = \frac{r_r}{r_{id}}.\dot{\theta}_r.(1-i) \tag{11}$$

where i is the slip between the vehicle wheel and rollers.

Substituting Eqs. (10) and (11) in Eq. (9):

$$F_{act} = \frac{1}{r_w}\cdot\left(T_b + T_{rr} + \left(J_w\cdot\frac{r_r}{r_w} + J_{id}\cdot\frac{r_w.r_r}{r_{id}^2}\right)\cdot(1-i)\cdot\ddot{\theta}_r\right) \tag{12}$$

From Eq. (12), a subsystem of action force F_{act} acting on the wheel can be built, as shown in Fig. 3(c).

To calculate friction force F_x, it requires the value of normal force because of the following expression:

$$F_m = \mu_p \cdot N \tag{13}$$

$$F_{xs} = \mu_s \cdot N \tag{14}$$

where F_{xm} and F_{xs} are maximum and sliding friction force, μ_p and μ_s are peak and sliding friction coefficient, and N is the normal force acting on rollers.

Because of the roller brake tester arrangement, the normal force acting on rollers is not the same as on a flat road. Its free-body diagram is shown in Fig. 4(a). From that figure, the normal force N can be expressed as:

$$N = \frac{W}{cos\left(\frac{\beta}{2}\right)} \tag{15}$$

where N is total normal force ($N_1 + N_2$), β is an angle formed by the normal force N_1 and N_2. W is the axle load acting on each wheel (tire normal load).

Substituting Eq. (15) in Eq. (13):

$$F_{xm} = \mu_p \cdot \frac{W}{\cos\left(\frac{\beta}{2}\right)}\,. \tag{16}$$

Based on Eq. (16), a roller brake tester has advantages and disadvantages. It can measure higher friction force than a flat plate with zero angle of β. The bigger the β, the higher the maximum friction force F_{xm} will be. It can be seen in Eq. (16) that the maximum friction force F_{xm} is inversely proportional to the cosine $\beta/2$.

The other advantage of a roller brake tester is the horizontal force, shown in Fig. 4(b). When a vehicle is tested and the driver presses the brake pedal, friction force F_{x1} and F_{x2} will arise on the contact between the tire tread and two rollers. Friction force on the non-tested wheel F_{rear} appears when the vehicle tends to move backwards. Friction force F_{rear} not always exists. It appears only in a specific condition.

From Fig. 4(c), it shows forces on the tested wheel to know when the vehicle tends to move backward, when the friction

force F_{rear} on the non-tested wheel exists, or when a retainer is required on the non-tested wheel. By taking a moment about point O in Fig. 4(c), the vehicle tends to move backwards or the normal force on roller 1 (N_1) reaches zero if the condition expressed in the following equation is true:

$$F_{x2}.r_w \geq N_{1y}.l \,. \tag{17}$$

The vertical component of normal force on roller 1 N_{1y} can be expressed as:

$$N_{1y} = \frac{W}{2} \,. \tag{18}$$

Using trigonometric, the length of l can be expressed as:

$$l = 2.r_w.sin\left(\beta/2\right) \,. \tag{19}$$

Substituting Eqs. (18) and (19) in Eq. (17):

$$F_{x2} \geq W.sin\left(\beta/2\right) \,. \tag{20}$$

Maximum friction force on roller 2 can be expressed as:

$$F_{x2\max} = \mu_p \cdot N_2 \,. \tag{21}$$

Based on Eq. (15), the normal force on roller 2 can be expressed as:

$$N_2 = \frac{1}{2}.\frac{W}{cos\left(\beta/2\right)} \,. \tag{22}$$

Substituting Eqs. (22) and (21) in Eq. (20):

$$\mu_p \geq \sin\beta \,. \tag{23}$$

Based on Eq. (23), the vehicle will not move backwards, or no retainer is required as long as:

$$\mu_p < \sin\beta \,. \tag{24}$$

According to Table 1, the value of the angle β is 58.2^0, and the peak friction coefficient μ_p is 0.7. Therefore, because the value of μ_p is less than sin β (0.85), the vehicle will never move backwards while testing is taking place. In other words, no need for a retainer attached to the non-tested wheel. The value of angle β depends on the distance between rollers, the roller diameter, and the effective radius of the tire. If a vehicle with a bigger tire radius is tested, it may move backwards because of the smaller angle β. Different from a brake tester proposed by Muthoriq et al., which always requires a retainer on the non-tested wheel to prevent the whole vehicle moves backward [36].

Despite its advantages, a roller brake tester has at least two weaknesses. The first one is also the effect of angle β as expressed in Eq. (16). In case of the action force of a wheel has the ability to overcome the maximum friction force ($F_{act} > F_{xm}$), the same vehicle will have different braking efficiency (maximum friction coefficient) if it is tested on different brake tester with different angle β according to Eq. (16). Hence, it can be concluded that as long as the angle β is different, the measurement result of a roller brake tester will not be precise. This is in accordance with the experiment conducted by Senabre et al. [24]. That experimentation shows that when a vehicle is tested in a roller brake tester with a higher angle β (longer distance between two rollers), the braking efficiency also increases.

The other weakness of a roller brake tester is its measurement accuracy. That is the main discussion in this paper. As shown in Fig. 1(a), the load cell measures the braking force (friction force) on the rollers surface indirectly. There is a long journey for the friction force before it reaches the load cell. The friction force is measured by the load cell through two rollers and gearbox assembly. Because of that, force detected by the load cell will be affected by the inertia of the roller and gearbox component. This complies with Xu et al., who state that the measurement error occurs because the braking force is transferred to a force transducer through two rollers, a floating transducer, a floating motor, and a floating measurement lever [27].

An electric motor used in a roller brake tester is a three-phase induction motor with a weakness. On an induction motor, the rotational speed is affected by its load. Hence, acceleration and deceleration of the roller cannot be avoided. Because of this, the inertia of rollers and gearbox components must be included in the calculation to increase accuracy. That is what has been done in this research.

After the calculation of action force F_{act} has been made, as shown in Fig. 3(c), the friction force F_x model can be built because F_x is a function of F_{act}. Modelling of F_x is shown in Fig. 5(a) with some assumptions. Before F_x reaches its peak value F_{xm}, the relationship between F_x and F_{act} is linear with a slope of 1 (point O-A). This is already known in basic friction when the system is at rest. After peak point A until sliding friction B are assumed to be linear with a slope of -1. This assumption is made because the tire is made from a flexible material. Finally, after point B is assumed to be constant where sliding or 100 % slip takes place.

Therefore, the curve in Fig. 5(a) can be expressed as:

For $F_{act} \leq F_{xm}$ (Point O-A):

$$F_x = F_{act} \,. \tag{25}$$

For $F_{act} \leq \left(2.F_{xm} - F_{xs}\right)$ (Point A-B):

$$F_x = 2.F_{xm} - F_{act} \,. \tag{26}$$

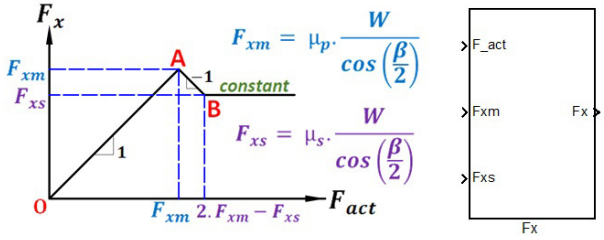

(a) (b)

Fig. 5. Model of friction force at roller surface F_x: (a) the curve of friction force F_x as a function of action force F_{act} acting on the wheel; (b) the subsystem of friction force F_x representing the curve in (a).

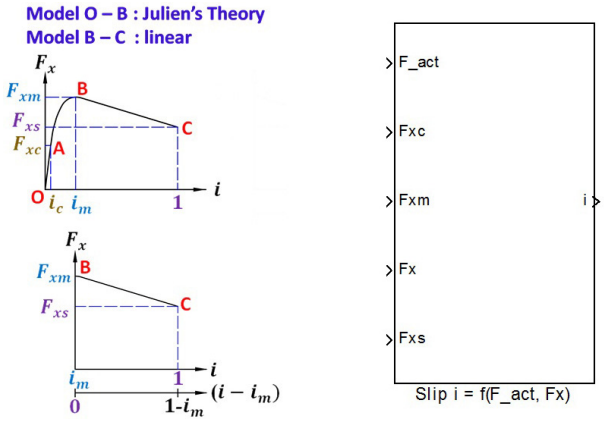

(a) (b)

Fig. 6. Model of slip i of the wheel: (a) slip characteristics curve of a tire. The top figure is a complete curve. The bottom figure is the curve after it reaches peak friction force and is modelled as a straight line; (b) a subsystem to calculate slip i based on (a).

For $F_{act} > (2.F_{xm} - F_{xs})$ (After B):

$$F_x = F_{xs} . \tag{27}$$

Based on Eqs. (25)-(27), a subsystem of friction force F_x can be built, as shown in Fig. 5(b).

As shown in Fig. 3(c), the action force F_{act} subsystem requires slip input, that is, slip between the tire and rollers. Therefore, a block diagram or subsystem calculating the slip value is needed. A curve for modelling slip i is shown in Fig. 6(a). Julien's theory was used to model the relationship between friction force F_x and slip i. Julien's theory only models from points O to B. Hence, points B-C will be modelled linear, as shown in Fig. 6(a) bottom.

Based on Julien's theory [8] and that assumption, equations used to make the curve in Fig. 6(a) can be expressed as:

For $F_{act} \le F_{xc}$ (Points O-A which is the adhesion region):

$$i = \frac{1}{K_t}.F_{act} \tag{28}$$

where:

$$K = k_t.l_t.\lambda \tag{29}$$

$$K_t = K.\left(1 + \frac{l_t}{2.\lambda}\right) \tag{30}$$

$$F_{xc} = \frac{\lambda.\left(1 + \frac{l_t}{2.\lambda}\right)}{(l_t + \lambda)}.F_{xm} \tag{31}$$

where k_t is the tangential stiffness of the tire, l_t is the length of the contact patch, λ is the length in front of the contact patch deformed, K_t is the initial slope of F_x vs i curve. F_{xc} is the critical friction force.

For $F_{act} \le F_{xm}$ (Point A-B, which is a combination of adhesion and sliding region):

$$i = \frac{b - \sqrt{b^2 - 4.a.c}}{2.a} \tag{32}$$

where:

$$a = K^2 \tag{33}$$

$$b = \frac{2.l_t.K}{\lambda}.(F_{xm} - F_{act}) + 2.F_{xm}.K \tag{34}$$

$$c = F_{xm}^2 . \tag{35}$$

For $F_{act} \le (2.F_{xm} - F_{xs})$ or point B-C made based on Fig. 6(a) bottom:

$$i = \frac{\left(1 - \frac{F_{xm}}{K}\right).(F_x - F_{xm})}{(F_{xs} - F_{xm})} + \frac{F_{xm}}{K} . \tag{36}$$

For $F_{act} > (2.F_{xm} - F_{xs})$ or after point C:

$$i = 1 . \tag{37}$$

Based on Eqs. (28)-(37), a subsystem of slip i can be built, as shown in Fig. 6(b).

2.2 Combining the models

Up to this point, four subsystems have been made: Roller, F_{act}, F_x, and slip i. If these subsystems are combined, as shown in Fig. 7(a), it results in a new subsystem, a roller brake tester, as shown in Fig. 7(b). That subsystem didn't include the measurement system of a real roller brake tester yet. Therefore, it is called the roller brake tester without load cell model. It has three inputs and some outputs. Its inputs are electric motor torque T_m, braking torque T_b, and rolling resistance torque T_{rr}. Its outputs are action force F_{act}, the friction force between rollers and the wheel F_x, speed of roller $\dot{\theta}_r$ and idler $\dot{\theta}_{id}$, slip i, and friction coefficient purely because of braking torque μ_{Tb}. The friction coefficient μ_{Tb} is calculated only to check the braking torque value and will not be connected to another sub-

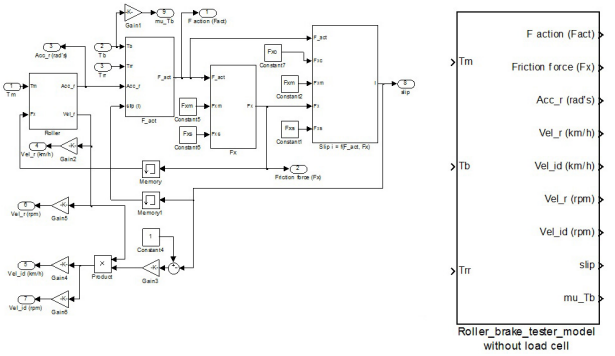

(a) (b)

Fig. 7. Model of roller brake tester without measurement system: (a) simulink® block diagram, which consists of roller, action force F_{act}, friction force F_x, and slip i subsystem; (b) subsystem of the roller brake tester made from block diagram in (a).

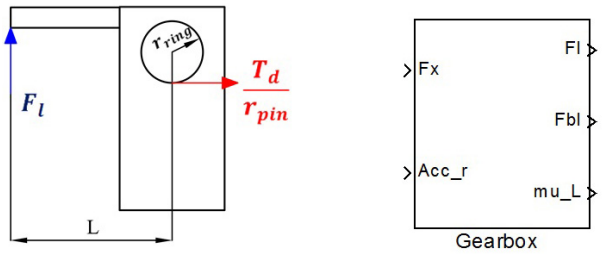

(a) (b)

Fig. 8. Model of gearbox assembly: (a) free body diagram; (b) the subsystem of the gearbox made from (a).

system.

The last step to complete the whole model of a roller brake tester is gearbox modelling. Assuming that the gearbox assembly is rigid, the force measured by the load cell based on the free body diagram in Fig. 8(a) and Eq. (3) can be expressed as:

$$F_l = \frac{1}{L}.\left(\left(J_{ring} + 2.J_r\right).\ddot{\theta}_r + F_x.r_r\right) \tag{38}$$

where F_l is the force measured by the load cell and L is the length of the gearbox lever.

On a roller brake tester, braking force or friction force is estimated with this formula [44]:

$$F_{bl} = \frac{L}{r_r}.F_l\,. \tag{39}$$

Friction coefficient or braking efficiency therefore can be expressed as:

$$\mu_l = \frac{F_{bl}}{W}\,. \tag{40}$$

From Eqs. (38)-(40), a subsystem of gearbox or measurement system can be built, as shown in Fig. 8(b).

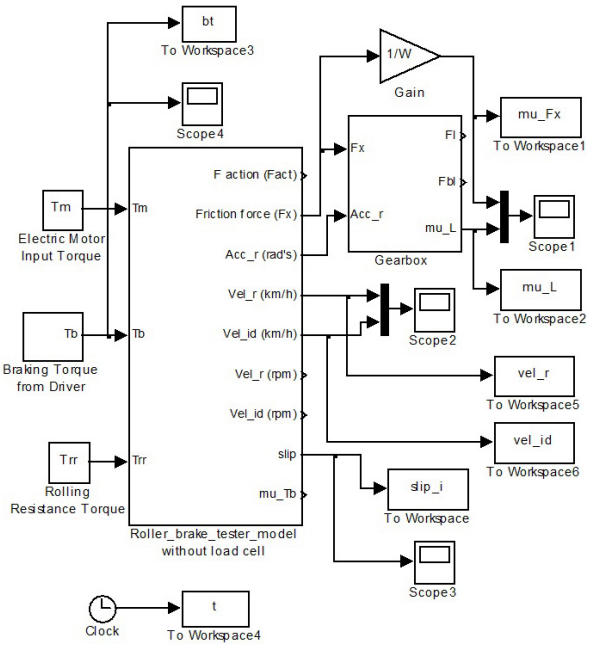

Fig. 9. Model of the current roller brake tester, which consists of the roller brake tester without measurement system (load cell) and the gearbox subsystem.

Model of a roller brake tester used today can be made by connecting the subsystem of the roller brake tester in Fig. 7(b) with the gearbox in Fig. 8(b), as shown in Fig. 9. Measurement output of a roller brake tester is friction coefficient or braking efficiency μ_l as in Eq. (40). This output will be compared with the true friction coefficient expressed as:

$$\mu_{Fx} = \frac{F_x}{W}\,. \tag{41}$$

A comparison between the friction coefficient measured by the brake tester μ_l and the actual friction coefficient μ_{Fx} will show the inaccuracy of a roller brake tester. The simulation was performed in three cases, i.e., 100 %, 25 %, and 2.5 % of slip. Data from a roller brake tester and tire parameters used for the simulation can be seen in Table 1.

Data in Table 1 are obtained from some sources. Electric motor torque is calculated from Eq. (2). Viscous damping and moment of inertia of the electric motor are obtained from simulation based on Eq. (1). Gearbox ratio is known from the calculation in such a way that the roller linear speed without load is about 5.5 km/h according to the brake tester specification [46]. The other parameters not available in references are determined based on proportional assumptions.

3. Method to improve accuracy by evaluating the brake tester rotational inertia

The basic idea to improve measurement accuracy is elimi-

Table 1. Roller brake tester and tire parameters.

Electric motor torque, T_m	35.7 N.m
Electric motor viscous damping, C_m	0.1137 N.m.s/rad
Electric motor moment of inertia, J_m	0.01 kg.m^2
Gearbox gear ratio ($r_{pin} : r_{ring}$)	1:24.67
Roller radius, r_r [45]	0.12 m
Wheel moment of inertia, J_w [45]	0.9 kg.m^2
Ring gear moment of inertia, J_{ring}	0.25 J_w
Roller moment of inertia, J_r	2 J_w
Wheel radius, r_w [45]	365 mm
Idler moment of inertia, J_{id}	0.25 J_w
Idler radius, r_{id}	0.25 r_{id}
Tire normal load, W [45]	4,675 N
Peak friction coefficient, μ_p [45]	0.7
Brake tester angle, β [45]	58.2^0
Sliding friction coefficient, μ_s	0.5
Rolling resistance coefficient, f_r	0.02
Lever length, L	0.5 m
Tangential stiffness of tire, k_t [6]	4610304 N/m^2
Contact patch length, l_t [6]	0.282 m
Length in front of contact patch deformed, λ [6]	0.0315 m

nating the influence of brake tester inertia. Hence, the rotational inertia must be identified first before testing a vehicle. Brake tester rotational inertia is estimated using curve fit (left division method of Matlab®) based on a second-order differential equation. That estimation is conducted after turning on the electric motor until constant speed without the vehicle wheel above the test rig. When testing a vehicle, the estimated inertia is used to calculate the friction force between the tire and the roller's surface. This way, brake tester measurement will be accurate, although the roller speed is not constant.

Based on Eq. (38), the inaccuracy of a roller brake tester is caused by the ring gear inertia J_{ring}, the roller inertia J_r, and the roller acceleration $\ddot{\theta}_r$. There are two ways to solve that problem. First, the speed of the roller is maintained to be constant. If its acceleration is zero, there will be no inertia. However, if the electric motor is an asynchronous type, the roller's speed will change when the wheel is braked.

The second way is by involving the effect of inertia in the calculation. Based on Eq. (38), an equation to eliminate the inertia and acceleration as a function of load cell measurement F_l can be expressed as:

$$F_{lc} = F_l - \frac{1}{L}.J_c.\ddot{\theta}_r \tag{42}$$

$$\text{where: } J_c = J_{ring} + 2.J_r \tag{43}$$

where F_{lc} is correction force based on the force measured by the load cell F_l, J_c is correction inertia which consists of the ring gear and rollers inertia.

Therefore, friction coefficient or braking efficiency after correction μ_{lc} (involving the effect of inertia) can be expressed as:

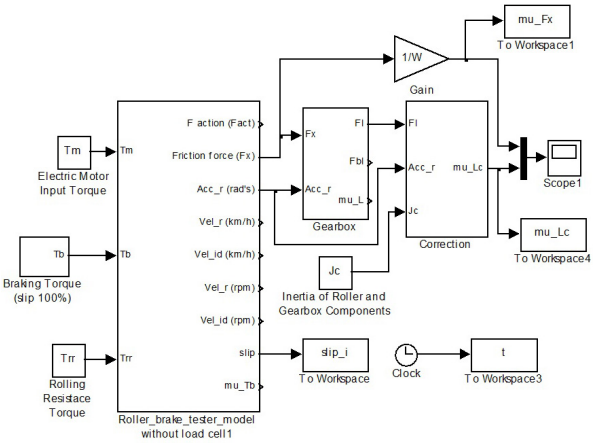

Fig. 10. The model of the modified roller brake tester. It consists of the roller brake tester without a measurement system (load cell), gearbox, and correction subsystem.

$$\mu_{lc} = \frac{F_{lc}}{W}. \tag{44}$$

Theoretically, the value of μ_{lc} will be the same as the friction coefficient μ_{Fx} in Eq. (41) as long as the value of J_c is accurate. Eq. (44) is used to simulate the effect of the correction method on a roller brake tester model.

A correction subsystem can be built based on Eqs. (42) and (44). It will be connected to the block diagram in Fig. 9 to prove that the coefficient of friction after correction μ_{lc} is similar to the actual friction coefficient μ_{Fx}. This combination is shown in Fig. 10.

As seen in Fig. 10, the correction subsystem requires inertia correction J_c, which consists of two rollers and ring gear inertia. The inertia J_c can be measured when no vehicle wheel is above the brake tester. It can be estimated using curve fit when the brake tester is started up. The left division method of MATLAB® can be used to do that [47]. An equation used to curve fit is based on Eq. (38) with zero F_x because there is no friction on the roller surface. The equation can be expressed in matrix form as:

$$\left[\ddot{\theta}_r\right].J_c = \left[F_l.L\right]. \tag{45}$$

Using the left division method, the value of J_c is:

$$J_c = \left[\ddot{\theta}_r\right] \backslash \left[F_l.L\right] \tag{46}$$

where $\left[\ddot{\theta}_r\right]$ is data of roller acceleration, $\left[F_l.L\right]$ is data of force measured by the load cell multiplied by the length of the lever. Those data are taken when the roller's speed is zero until the steady state. In reality, it requires a speed sensor attached

to the roller. Data on roller acceleration is obtained by differentiating the data of roller speed once.

The block diagram in Fig. 9 was used to perform a simulation for measuring the inertia J_c. Simulation without the vehicle wheel can be done by setting the friction force F_x, rolling resistance T_{rr}, and braking torque T_b equal to zero.

4. Simulation results and discussions

The existing and modified roller brake tester were simulated using the block diagram in Figs. 9 and 10, respectively. With those simulation results, factors that contribute to measurement error can be identified.

4.1 Simulation of the current roller brake tester

A simulation of 100 % slip is shown in Fig. 11. To make the wheel 100 % slip requires braking torque in Fig. 11(a). In the simulation, the driver of a vehicle presses the brake pedal after the time is 2 seconds. How the wheel slips can be seen in Fig. 11(c), which shows the speed of the idler reaches zero. The idler speed represents the speed of the wheel. Hence, the percentage of the linear speed difference between the idler and roller is called slip. From Fig. 11(c), the minimum speed of the roller is about 3.25 km/h. That value conforms with the requirement of a roller brake tester. The speed of the rollers has to be in the range of 2-5.5 km/h when testing is taking place [46]. The comparison between the brake tester measurement and the actual value can be seen in Figs. 11(b) and (d).

Simulations of 25 % and 2.5 % slip are shown in Figs. 12 and 13. These simulations are conducted to take a closer look at small slip where the wheel or rollers has the most significant deceleration. To do that, braking torque lower than those of 100 % slip are given, as can be seen in Figs. 12(a) and 13(b). Similar to 100 % slip, the comparison of the true and brake tester measurements are shown in Figs. 12(b), (d) and 13(b), (d). Slip between the vehicle wheel (idler) and roller are shown in Figs. 12(c) and 13(c).

4.2 Simulation of the modified roller brake tester/ proposed method

There are two steps to simulate the proposed method. The first one is rotational inertia estimation. It is conducted using a block diagram in Fig. 9 but without the vehicle wheel (braking torque, rolling resistance, and friction force equal to zero). Data to be observed are force measured by the load cell and roller speed when the electric motor is turned on until steady, as seen in Figs. 14(a) and (b). Based on these data, the inertia of the brake tester components can be estimated.

The second one is the simulation of tire testing after the brake tester rotational inertia is identified in the first step. This simulation uses the block diagram in Fig. 10, which involves the brake tester inertia J_c for correction. Simulation results are friction coefficient and slip characteristics curve as shown in Figs. 14 (c) and (d).

4.3 Discussion

Based on Figs. 11(b) and (c), the brake tester measurements are inaccurate in some points. When there is acceleration or deceleration of the roller, the measurement will not be the same as the actual value. If the roller's speed increases, the brake tester measurement will be higher than the true value. On the contrary, if the roller's speed decreases, the brake tester measurement will be lower than the true value. At the beginning of the simulation, when the time is less than 1 second or the linear velocity of the roller increases, the total friction force acting on two roller's surfaces is caused by the wheel inertia, the idler inertia, and the rolling resistance of the wheel. How-

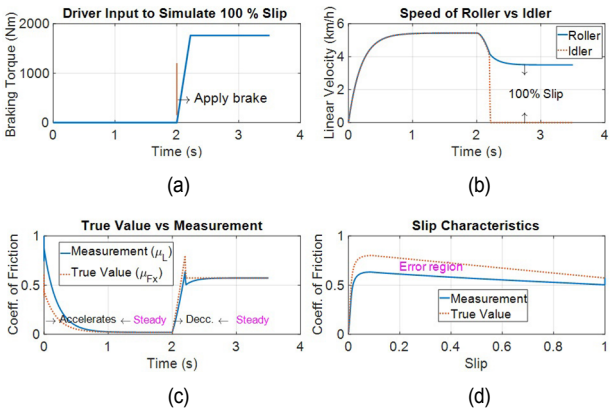

Fig. 11. Simulation of 100 % slip: (a) braking torque input from vehicle driver to produce 100 % slip; (b) comparison of the true friction coefficient μ_{Fx} and friction coefficient measured by the brake tester μ_l; (c) the linear velocity of the roller and idler; (d) comparison of the true slip characteristics and slip characteristics measured by the brake tester.

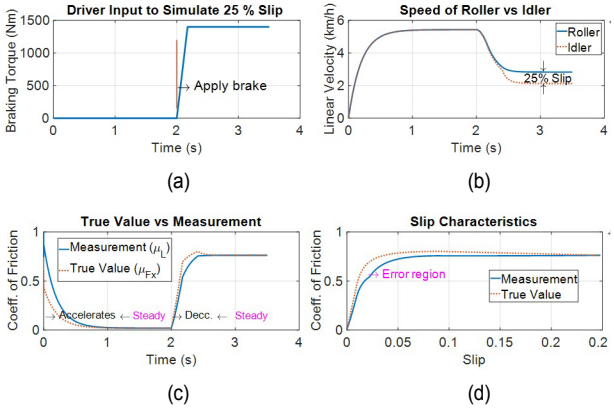

Fig. 12. Simulation of 25 % slip: (a) braking torque input from vehicle driver to produce 25 % slip; (b) comparison of the true friction coefficient μ_{Fx} and friction coefficient measured by the brake tester μ_l; (c) the linear velocity of the roller and idler; (d) comparison of the true slip characteristics and slip characteristics measured by the brake tester.

ever, the brake tester measures not only these inertias and rolling resistance but also the inertia of two rollers and the inertia of the ring gear of the gearbox assembly, as can be seen in Eq. (38). That is why the brake tester measurement is higher than the actual value.

At the time more than 2 seconds or after the brake pedal of a vehicle is pressed, the measurement is lower than the true value. That is because the roller is in deceleration mode, as shown in Fig. 11(c), after 2 seconds. When the roller decelerates, the inertia of the rollers and ring gear will reduce the force measured by the load cell. Hence, the friction coefficient measured by the brake tester will be lower than the actual friction coefficient on the roller's surface. This phenomenon complies with the experiment conducted by Firdaus et al. [48]. Their investigation shows that the braking efficiency in fluctuating braking is lower (40 %) than in gradual braking (44 %). When intermittent braking is applied, the roller's deceleration will be higher than gradual braking. Therefore, higher inertia will reduce the force sensed by the load cell.

When the speed of the roller is constant, the measurement is accurate. It can be seen in Figs. 11(b) and (c). In the time between 1-2 seconds and after 2.5 seconds, the brake tester measurement is the same as the actual value. That is because when there is no acceleration, the inertia will be zero. In short, the measurement of a roller brake tester is accurate only if the roller's speed is in a steady state.

Based on that explanation, if the slip characteristics curve is plotted, the brake tester will not give an accurate result, as shown in Fig. 11(d). The curve from the brake tester measurement will be lower than the true value. That figure is plotted from 1 second until 3.5 seconds. The slip of the wheel used as an axis is known by calculating the difference between the linear velocity of the idler and roller. Obtaining the slip data on a roller brake tester requires a speed sensor attached to one roller and the idler.

The 25 % and 2.5 % slip simulation in Figs. 12 and 13 shows the same phenomenon as the simulation of 100 % slip. The measurement is correct if the speed of the roller doesn't change. These simulations are conducted to zoom in on the slip characteristic curve. The zoom-in of slip characteristics from 0 to 25 % and 0 to 2.5 % are seen in Figs. 12(d) and 13(d), respectively.

From Figs. 12(d) and 13(d), it can be seen that the measurement is accurate only in two points. These are a point where the slip is zero and the point where the maximum slip is reached. Between those two points, the friction coefficient measured by the brake tester is lower than the actual value. As discussed before, that is because the slip characteristic curve is plotted after 1 second where the roller is in deceleration after a steady state. When the speed of the roller decreases, roller and ring gear inertia will reduce the force acting on the load cell. Therefore, the force measured by the load cell will be lower than the friction force acting on the roller surface. Paulo et al. also state that the force transducer of a roller brake tester measures not only the friction force on the roller surface but also parasite forces (inertia of rollers, a wheel, and the transmission system) [26].

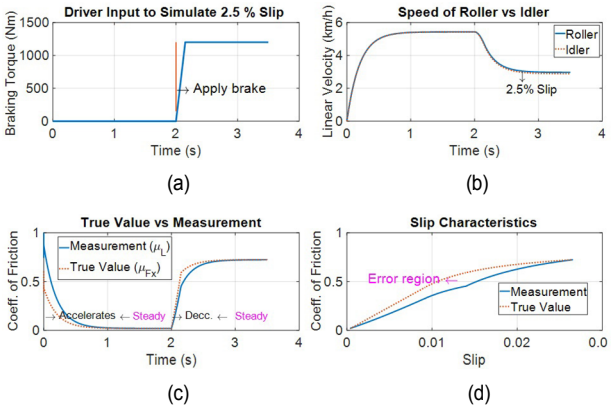

Fig. 13. Simulation of 2.5 % slip: (a) braking torque input from vehicle driver to produce 2.5 % slip; (b) comparison of the true friction coefficient μ_{Fx} and friction coefficient measured by the brake tester μ_l; (c) the linear velocity of the roller and idler; (d) comparison of the true slip characteristics and slip characteristics measured by the brake tester.

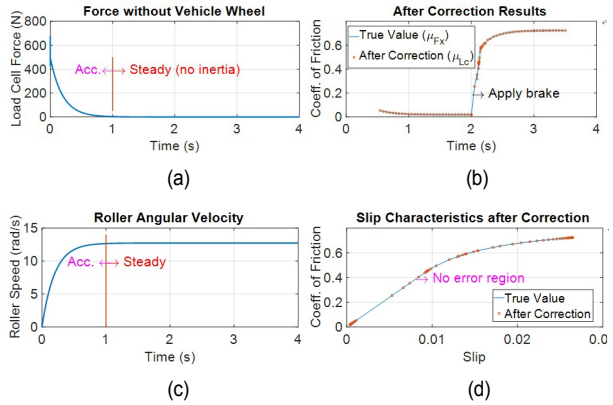

Fig. 14. Simulation results of the roller brake tester without vehicle wheel: (a) force measured by the load cell; (b) angular velocity of the roller. Simulation results of the roller brake tester after applying correction method (involving the inertia of rollers and ring gear J_c); (c) comparison of true friction coefficient and friction coefficient of the brake tester after correction; (d) comparison of tire slip characteristics between true value and brake tester measurement after correction.

Because the measurement is only accurate when the roller is in a steady state, a roller brake tester used today cannot be used to measure/model the tire characteristics. To make it possible, we proposed a method to increase the accuracy. Before conducting testing, the inertia correction J_c must be known. That inertia is measured when no vehicle wheel is above the brake tester. The block diagram in Fig. 9 was used to do the simulation. Data of force measured by the load cell and the roller's speed is shown in Figs. 14(a) and (b). Based on Figs. 14(a) and (b), by using Eq. (46), the estimated value of J_c is 3.8378 kg.m^2. The real value of J_c from Table 1 is 3.8250 kg.m^2, which consists of two roller inertia and ring gear inertia, as in Eq. (43).

After the inertia correction J_c has been identified, the brak-

ing system testing of a vehicle can be started. The block diagram in Fig. 10 was used to simulate that testing. It compares the actual value with the brake tester measurement after involving the inertia correction J_c. The simulation results are shown in Figs. 14(c) and (d). From Fig. 14(c), it can be seen that the friction coefficient value from the brake tester measurement after correction is accurate in all points. Therefore, plotting the tire's slip characteristic becomes accurate, as shown in Fig. 14(d).

These results show that the method proposed can be used to improve the accuracy of the measurement system of a roller brake tester. Therefore, the modified roller brake tester can measure the maximum friction coefficient or braking efficiency and model the tire.

5. Conclusions

Based on the simulation, by adding just two speed sensors installed on one roller and the idler, the accuracy of a roller brake tester had been improved. First, the inertia correction J_c was estimated using curve fitting when no vehicle wheel was above the test bench. Data used for curve fitting were the speed of the roller and force measured by the load cell. These data were taken from zero speed until steady state. The inertia correction value J_c was then used to calculate the friction coefficient based on the force measured by the load cell. The simulation showed that after involving inertia correction J_c in the calculation, the effect of inertia was diminished. The measurement of the roller brake tester became accurate in all points from zero slip until maximum slip, unlike the current brake tester which is only accurate when the speed of the rollers is constant. Hence, by this simple method, a roller brake tester could be used not only to measure maximum braking efficiency but also to test/model the tire.

From mathematical modelling, the angle β formed by normal forces of two rollers gives measurement characteristics. Suppose the braking system output of a vehicle is more than the maximum friction force between the roller surface and the tire. In that case, the same vehicle will have different maximum braking efficiency if tested on different brake testers with different values of β. The bigger the angle, the higher the maximum friction force will be. In addition, the angle β will determine whether the vehicle moves backwards during testing. If the peak friction coefficient between the tire and the roller surface equals or exceeds the value of sine β, the vehicle will move backwards. Therefore, if that condition happens, it requires a retainer installed on the non-tested wheel.

Acknowledgments

This work was supported by The Indonesian Endowment Funds for Educational/Lembaga Pengelola Dana Pendidikan/LPDP (No. 201701210110284). The authors also thank Politeknik Keselamatan Transportasi Jalan (PKTJ) of Ministry of Transportation for providing data of a roller brake tester.

Nomenclature

$\ddot{\theta}_{id}$: Idler angular acceleration
$\dot{\theta}_{id}$: Idler angular velocity
$\ddot{\theta}_{m}$: Electric motor shaft angular acceleration
$\dot{\theta}_{m}$: Electric motor shaft angular velocity
$\ddot{\theta}_{r}$: Roller angular acceleration
$\dot{\theta}_{r}$: Roller angular velocity
$\ddot{\theta}_{w}$: Wheel angular acceleration
$\dot{\theta}_{w}$: Wheel angular velocity
μ_{Fx} : True friction coefficient/braking efficiency
μ_{I} : Friction coefficient/braking efficiency estimated by the existing brake tester
μ_{Ic} : Friction coefficient/braking efficiency estimated by the modified roller brake tester
μ_{p} : Peak friction coefficient between roller surface and tire
μ_{s} : Sliding friction coefficient between roller surface and tire
C_{m} : Electric motor viscous damping
F_{act} : Action force acting on the vehicle wheel consists of braking torque, rolling resistance torque, and inertia of the wheel and idler
F_{bI} : Braking force/friction force estimated by the existing roller brake tester
F_{I} : Force measured by load cell
F_{Ic} : Friction force/braking force estimated by the modified roller brake tester
F_{rear} : Friction force on non-tested wheel
F_{x} : Total friction force on roller 1 and 2
F_{x1} : Friction force acting on roller 1
F_{x2} : Friction force acting on roller 2
F_{x2max} : Maximum friction force on roller 2
F_{xm} : Maximum friction force on roller surface
F_{xs} : Sliding friction force on roller surface
J_{c} : Correction inertia consists of ring gear and rollers inertia
J_{id} : Idler moment of inertia
J_{m} : Electric motor moment of inertia
J_{r} : Roller moment of inertia
J_{ring} : Ring gear moment of inertia
J_{tot} : Total inertia consists of electric motor, ring gear, and roller inertia
J_{w} : Wheel moment of inertia
N_{1} : Normal force acting on roller 1
N_{1y} : Vertical component of normal force on roller 1
N_{2} : Normal force acting on roller 2
T_{b} : Braking torque
T_{d} : Electric motor load torque
T_{m} : Electric motor torque
T_{rr} : Rolling resistance torque
T_{w1} : Roller 1 torque
T_{w2} : Roller 2 torque
r_{id} : Idler radius
r_{pin} : Pinion gear effective radius
r_{r} : Roller radius
r_{ring} : Ring gear effective radius
r_{w} : Wheel effective radius

L : Length of gearbox lever
N : Total normal force of roller 1 and 2
W : Heel/tire normal load
i : Slip between vehicle wheel and roller
β : Angle formed by two normal forces acting on roller 1 and 2

Tire parameters (Julien's theory)

F_{xc} : Critical friction force
K_t : Initial slope of friction force vs slip curve
k_t : Tangential stiffness of tire
l_t : Length of contact patch
λ : Length in front of contact patch deformed

References

[1] H. Yamashita, Y. Matsutani and H. Sugiyama, Longitudinal tire dynamics model for transient braking analysis: ANCF-LuGre tire model, *J. Comput. Nonlinear Dyn*., 10 (3) (2015) 1-11.

[2] H. Hong, G. Kim, H. Lee, J. Kim, D. Lee, M. Kim, M. Suh and J. Lee, Optimal location of brake pad for reduction of temperature deviation on brake disc during high-energy braking, *J. Mech. Sci. Technol*., 35 (3) (2021) 1109-1120.

[3] B. Hu, X. Zhang, Y. Liu, J. Yan, X. Liu, X. Wang and R. Sun, 3D quasi-transient thermo-mechanical analysis for vehicle brake disc, *J. Mech. Sci. Technol*., 36 (2) (2022) 969-981.

[4] L. Romano, A. Sakhnevych, S. Strano and F. Timpone, A novel brush-model with flexible carcass for transient interactions, *Meccanica*, 54 (10) (2019) 1663-1679.

[5] R. Hadekel, *The Mechanical Characteristics of Pneumatic Tires*, National Association of Housing & Redeve (1952).

[6] A. N. De Oliveira, C. G. Campos, A. O. Peralta, R. T. D. C. Neto and A. B. Caldeira, Parameters estimation of a tire model based on Julien's theory, *SAE Tech. Pap*. (2017) 2017-36-0177.

[7] H. B. Pacejka and I. J. M. Besselink, Magic formula tyre model with transient properties, *Veh. Syst. Dyn*., 27 (1997) 37-41.

[8] J. Y. Wong, *Theory of Ground Vehicles*, 4th Ed., John Wiley & Sons, Canada, USA (2008).

[9] L. Romano, F. Timpone, F. Bruzelius and B. Jacobson, Analytical results in transient brush tyre models: theory for large camber angles and classic solutions with limited friction, *Meccanica*, 57 (1) (2022) 165-191.

[10] B. Li, X. Yang and J. Yang, Out-of-plane flexible ring tyre model development and validation, *Int. J. Veh. Perform*., 7 (2021) 83-119.

[11] B. Li, X. Yang and J. Yang, Development of an out-of-plane flexible ring tire model compared with commercial FTire® via virtual cleat tests, *SAE Tech. Pap*. (2018) 2018-01-1120.

[12] M. Kane and V. Edmondson, Tire/road friction prediction: introduction a simplified numerical tool based on contact modelling, *Veh. Syst. Dyn*., 60 (3) (2022) 770-789.

[13] G. L. Gissinger, Y. Chamaillard and T. Stemmelen, Modelling a motor vehicle and its braking system, *Math. Comput. Simul*., 39 (1995) 541-548.

[14] J. Wu, Q. Wang, X. Wei and H. Tang, Studies on improving vehicle handling and lane keeping performance of closed-loop driver-vehicle system with integrated chassis control, *Math. Comput. Simul*., 80 (12) (2010) 2297-2308.

[15] Y. Pan, X. Nie, Z. Li and S. Gu, Data-driven vehicle modeling of longitudinal dynamics based on a multibody model and deep neural networks, *Meas. J. Int. Meas. Confed*., 180 (2021).

[16] X. Wang and Y. Cheng, Lane departure avoidance by man-machine cooperative control based on EPS and ESP systems, *J. Mech. Sci. Technol*., 33 (6) (2019) 2929-2940.

[17] V. K. T. Mantripragada and R. Krishna Kumar, Sensitivity analysis of tyre characteristic parameters on ABS performance, *Veh. Syst. Dyn*., 60 (1) (2022) 47-72.

[18] M. Guiggiani, *The Science of Vehicle Dynamics*, 2nd Ed., Springer Nature, Switzerland (2018).

[19] J. A. Cabrera, J. J. Castillo and P. Hern, A procedure for determining tire-road friction characteristics using a modification of the magic formula based on experimental results, *Sensors*, 18 (896) (2018) 1-17.

[20] M. A. Salama, V. V. Vantsevich, T. R. Way and D. J. Gorsich, UGV with a distributed electric driveline : controlling for maximum slip energy efficiency on stochastic terrain, *J. Terramechanics*, 79 (2018) 41-57.

[21] C. Senabre, E. Velasco and S. Valero, Variability of data when testing the handbrake parking system vs the electronic park brake with three maha testers at ministry of transport facilities, *Arch. Ind. Eng*., 2 (3) (2018) 1-8.

[22] C. Senabre, E. Velasco and S. Valero, Wheel diameter and width influence in variability of brake data measurement at Ministry of transport facilities, *Int. J. Mech. Mechatronics Eng*., 10 (4) (2016) 819-823.

[23] C. Senabre, E. Velasco and S. Valero, A hole in the vacuum hose of a vehicle provides lower differences in brake measurements by the ministry of transport brake testers rather than the characteristics of the tester used, *Mechanika*, 24 (2) (2018) 284-288.

[24] C. Senabre, E. Velasco and S. Valero, Comparative analysis of various brake testers used in ministry of transport facilities, such as: bank of roller testers and dynamometric platform testers, *Adv. Automob. Eng*., 4 (2) (2015) 2-7.

[25] J. Li, X. Zha and D. Wu, The theoretical analysis of test result's errors for the roller type automobile brake tester, *Computer and Computing Technologies in Agriculture IV. CCTA 2010. IFIP Advances in Information and Communication Technology*, 347 (2011) 382-389.

[26] P. L. S. Ferreira, P. R. G. Couto, L. C. Cabral, R. G. Reis and M. Zillner, A proposal for dynamic calibration of brake tester, *J. Phys. Conf. Ser*., 648 (1) (2015).

[27] G. Xu, J. Su, R. Chen, H. Pan, L. Zhang and X. Wang, Measurement performance assessment: dynamic calibration compared with static calibration method for roller tester of vehicle brake force, *Adv. Mech. Eng*. (2014) https://doi.org/10.1155/2014/162435.

[28] S. G. Tilden, S. Manor and L. I. N.Y, *Motor Vehicle Brake Testing Device*, US Patent No.: 2.079.751 (1937).

[29] J. N. Rogers, J. M. Lady, D. W. Bilsbarrow and R. S. Trujillo,

Vehicle Brake Test System, US Patent No.: 4893242 (1990).
[30] S. Ishizeki, *Method of Testing an Anti-Lock Brake Control System of a Motor Vehicle*, US Patent No.: 5.005.405 (1991).
[31] H. Wimmer, *Test Stand for Motor Vehicle*, US Patent No.: US 7.392.693 B2 (2008).
[32] E. Seibl, *Roller Brake Testing Dynamometer*, US Patent No.: US 7.752.903 B2 (2010).
[33] Z. Li, F. Zuo, X. M. Dong and J. Xiao, *Counter-Force Type Roller Braking Test Bed with Adjustable Center Distance*, Patent No.: CN210090038U (2019).
[34] Z. C. Liao, X. X. 'Frank' Bai, Y. Li, X. C. Deng and J. Sun, Design, modeling, and verification of a test bench for braking simulation of 1/4 vehicle, *Proc. Inst. Mech. Eng. Part D J. Automob. Eng.*, 234 (5) (2020) 1425-1441.
[35] O. S. Yan'kov, A. S. Chernyshkov, M. V. Kornyakov and A. V. Gilev, Experimental study of metrological properties of magnetostrictive sensors when changing their design parameters, *IOP Conf. Ser. Mater. Sci. Eng.*, 632 (1) (2019).
[36] E. Muthoriq, Z. Abidin, A. Hariyanto and M. Bur, A method for measuring tire characteristic using brake tester, *IOP Conf. Ser. Mater. Sci. Eng.*, 788 (1) (2020).
[37] E. Olmeda, M. Garrosa, S. S. Sánchez and V. Díaz, Development and characterization of a compact device for measuring the braking torque of a vehicle, *Sensors (Switzerland)*, 20 (15) (2020) 1-14.
[38] C. Senabre, E. Velasco and S. Valero, Self-organizing maps for identification of tire model longitudinal braking parameters of a vehicle on a roller brake tester and on flat ground, *Neural Comput. Appl.*, 21 (7) (2012) 1775-1782.
[39] C. Senabre, E. Velasco and S. Valero, Comparative analysis of vehicle brake data in the ministry of transport test on the roller brake tester and on flat ground, *Int. J. Automot. Technol.*, 13 (5) (2012) 735-742.
[40] H. Öktem, I. Uygur and M. Çevik, Design, construction and performance of a novel brake pad friction tester, *Meas. J. Int. Meas. Confed.*, 115 (2018) 299-305.
[41] J. J. Eckert et al., Experimental evaluation of rotational inertia and tire rolling resistance for a twin roller chassis dynamometer, *SAE Tech. Pap.* (2017) 2017-36-0212.
[42] M. A. de M. Lourenço, J. J. Eckert, F. L. Silva, F. M. Santiciolli and L. C. A. Silva, Vehicle and twin-roller chassis dynamometer model considering slip tire interactions, *Mech. Based Des. Struct. Mach.* (2022) 1-18.
[43] T. Rai and P. Debre, Generalized modeling model of three phase induction motor, *Int. Conf. Energy Effic. Technol. Sustain. ICEETS 2016*, Nagercoil, India (2016) 927-931.
[44] T. Skreblin, Roller brake tester measurement uncertainty calculation, *17th IMEKO TC 10 and EUROLAB Virtual Conference "Global Trends in Testing, Diagnostics & Inspection for 2030"* (2020) 326-331.
[45] H. Pan et al., The model and simulation analysis for the detection performance of brake tester, *2011 International Conference on Electrical and Control Engineering*, Yichang, China (2011) 3250-3253.
[46] CVRT (Commercial Vehicle Roadworthiness Testing), *Light Commercial Vehicle Roller Brake Tester (RBT)*, CVRT.
[47] W. J. Palm III, *A Concise Introduction to Matlab*, McGraw-Hill, New York, USA (2008).
[48] R. M. Firdaus, B. Supriyo and A. Suharjono, Analysis of braking force efficiency measurements for various braking strategy applied for vehicle tested on roller brake tester, *J. Phys. Conf. Ser.*, 1517 (1) (2020).

Ery Muthoriq received B.Eng. in mechanical engineering from Sebelas Maret University, Indonesia, in 2007 and M.Eng. from Institut Teknologi Bandung, Indonesia, in 2013. He is currently a doctoral degree candidate in mechanical engineering at Institut Teknologi Bandung, Indonesia. His research interest mainly focus on brake testing, vehicle dynamics, and system modelling.